communications earth & environment

ARTICLE

https://doi.org/10.1038/s43247-021-00333-1 OPEN

# The global carbon sink potential of terrestrial vegetation can be increased substantially by optimal land management

Zongyao Sha[1], Yongfei Bai[2], Ruren Li[3], Hai Lan[4], Xueliang Zhang[5], Jonathon Li[6], Xuefeng Liu[7], Shujuan Chang[8] & Yichun Xie[9]✉

Excessive emissions of greenhouse gases — of which carbon dioxide is the most significant component, are regarded as the primary reason for increased concentration of atmospheric carbon dioxide and global warming. Terrestrial vegetation sequesters 112–169 PgC (1PgC = $10^{15}$g carbon) each year, which plays a vital role in global carbon recycling. Vegetation carbon sequestration varies under different land management practices. Here we propose an integrated method to assess how much more carbon can be sequestered by vegetation if optimal land management practices get implemented. The proposed method combines remotely sensed time-series of net primary productivity datasets, segmented landscape-vegetation-soil zones, and distance-constrained zonal analysis. We find that the global land vegetation can sequester an extra of 13.74 PgC per year if location-specific optimal land management practices are taken and half of the extra clusters in ~15% of vegetated areas. The finding suggests optimizing land management is a promising way to mitigate climate changes.

[1] School of Remote Sensing and Information Engineering, Wuhan University, Wuhan, China. [2] Institute of Botany, Chinese Academy of Sciences, Beijing, China. [3] School of Transportation Engineering, Shenyang Jianzhu University, Shenyang, China. [4] Department of Geographical Sciences, University of Maryland, College Park, MD, USA. [5] School of Urban and Regional Science, Shanghai University of Finance and Economics, Shanghai, China. [6] Department of Geography & Environmental Management, University of Waterloo, Waterloo, Canada. [7] School of Communication and Information Engineering, Shanghai University, Shanghai, China. [8] Inner Mongolian Forestry & Rangeland Monitoring and Planning Institute, Hohhot, China. [9] Department of Geography and Geology, Eastern Michigan University, Ypsilanti, MI, USA. ✉email: yxie@emich.edu

Keeping the global temperature increase below 1.5 °C in accord with the Paris Agreement would require prompt and substantial reductions in greenhouse gases (GHGs) emissions on the global scale[1]. Despite considerable effort internationally, many countries are likely to miss the emission control targets proposed in the Paris Agreement. The world is on track for more than 3 °C of warming by the end of the century[2,3]. Numerous policies have long been proposed to cut down GHGs emissions, including resorting to renewable energy, popularizing electric vehicles, optimizing land-use policies, as well as other GHGs cutting policies or programs[1,4]. Unfortunately, those policy options seem not being effectively deployed, given the continuous increase of the emissions of GHGs[5,6]. The atmospheric $CO_2$ has risen beyond 400 ppm in recent years, which is attributed to carbon emissions from fossil fuel combustion and explains the 1.5 °C increase in air temperature since the 1880s[7,8].

Though cutting fossil fuel consumption provides a direct option to reduce carbon emissions, it shows limited effect in mitigating atmospheric $CO_2$ because fossil energy still powers the economy in many countries[4,9]. Vegetation dominates most terrestrial ecosystems (e.g., forests, grasslands, croplands, shrublands, and savannas) and absorbs 112–169 PgC each year from the atmosphere through a biochemical process called photosynthesis[8,9]. Improving vegetation carbon sequestration provides an alternative measure to counteract the excessive carbon emissions[9,10]. The net amount of carbon captured by plants through photosynthesis over a given period is called net primary production (NPP)[11,12]. NPP is closely related to a carbon sink, which is equivalent to NPP minus the component of soil heterotrophic respiration[13]; thus, NPP serves as a good proxy for evaluating carbon sink. As a key component of energy and mass transformation in terrestrial ecosystems, NPP depends on various factors, such as the supply of nutrients, water availability, soil profile characteristics, and landscape attributes (e.g., terrain and drainage)[14,15]. Those factors can be broadly categorized as the following three groups[16]: (1) climate impact (e.g., precipitation and temperature); (2) nonclimatic natural factors such as soil property, landforms, and biomes; and (3) human-related (HUMAN) land-management practices.

First, vegetation will not attain the saturation of carbon sequestration capacity without appropriate climatic conditions[10]. Lack of rainfall causes physiological stress and limits vegetation photosynthesis in most arid regions[14]. The dependence of vegetation carbon sequestration on climatic factors is reflected by most NPP models[11]. For example, the climate-driven Miami model, which has been widely applied to map large-scale NPP[10,17,18], highlights the climatic factors' importance as vital drivers to carbon sequestration. Second, vegetation cannot maximize carbon sequestration without favorable natural conditions such as landforms[15], soil properties[19], and biome groups[10]. Lastly, carbon sequestration can be updated by land-management practices (LMPs)[9], i.e., one LMP may result in higher or lower carbon sequestration than the other, under the same environmental contexts (the climatic and nonclimatic conditions).

Previous studies confirm that land use and management strategies have a massive effect on carbon sequestration from vegetation[18,20,21]. An optimal land-management practice (OLMP) refers to an LMP that helps sequester higher, if not the highest, potential carbon from the managed vegetation given the current climatic, nonclimatic, and HUMAN conditions. Once LMPs are replaced with OLMPs, the vegetation will sequester more carbon. It is valuable to model the difference in carbon sequestration between with and without OLMPs, called carbon gap hereafter, to make smart land-management policies and mitigate global climate changes. In a broad sense, OLMPs include removing negative human-related disturbances in naturally vegetated areas[21], and applying human-intervened programs/practices that help improve vegetation productivity or restore previously degraded vegetation[22,23]. The United Nations Convention to Combat Desertification program introduces over 1000 sustainable land-management practices based on the type of activities targeting to promote agricultural production while simultaneously supporting the environmental functions[24]. OLMPs include but are not limited to sustainable land-management practices, considering that all existing LMPs could be potentially selected as OLMPs if they help enhance vegetation productivity. For example, appropriate tillage practices on cropland may increase agricultural production (which in most cases also improves NPP); similarly, protection measures for trees close to road networks are necessary to improve forestry NPP[25]. Some cases of OLMPs are illustrated in Supplementary Table 1. The impact of OLMPs on vegetation productivity pertains to local environmental and socio-economical contexts. The carbon gap of specific OLMPs can be evaluated by comparing NPP of field experiments with and without the OLMPs implemented. Because the global natural and socioeconomic contexts exhibit manifest spatial variations, there are no universally applicable OLMPs. There is also a need for mapping carbon gaps through a globally and locally consistent approach so that both global comparison and local policy enactment are supported[26]. This work addresses the following questions: how much more carbon (i.e., carbon gap) could be further sequestered from global terrestrial vegetation with OLMPs implemented? How can the location-dependent OLMPs be decided from the local contexts at each location? Where do the most sensitive areas showing carbon sequestration improvement locate?

## Results

**Global carbon gap modeling and mapping**. The temporally averaged total carbon gap (during 2001–2018) for the vegetated land area is estimated to be 13.74 PgC $yr^{-1}$, with a spatially averaged carbon gap flux density of 124.3 gC $m^{-2}$ $yr^{-1}$ (Supplementary Table 2). Considering that the terrestrial NPP totaled 67.90 PgC $yr^{-1}$, ~1/5 more carbon can be added to the existing vegetation carbon sequestration if OLMPs are implemented. It was reported that the global fossil fuel emissions in 2019 were about 10.1 ± 0.6 PgC[4]. When the ratio of soil heterotrophic respiration ($R_H$) to NPP is about 0.71~0.74 (see "Methods"), the total carbon gap of 13.74 PgC $yr^{-1}$ means reducing an extra 3.5~4.0 PgC $yr^{-1}$ from the atmosphere and compensating more than 1/3 of the global fossil fuel emissions. Fossil $CO_2$ emissions in China, the United States of America (USA), and the European Union (EU28) contribute more than half of the global total, amounting to 2.75, 1,47, and 0.93 PgC in 2018, respectively[4]. Our analysis reveals that China, USA, and the EU28 could sequester an extra 0.29–0.32, 0.40–0.45, and 0.26–0.29 PgC in 2018 from the atmosphere by introducing OLMPs, accounting for 11–12%, 28–31%, and 27–31% of the fossil $CO_2$ emissions, respectively.

The terrestrial carbon gap flux showed significant spatial variations (Fig. 1). Locations with higher carbon gap density indicate that their current LMPs are highly recommended to be replaced with the OLMPs identified from their neighborhoods, aiming to improve NPP and thus narrow down the carbon gap. OLMPs could take different forms depending on the local environmental and social conditions (with typical examples illustrated in Supplementary Table 1). The above-mentioned LMPs, if proved to be effective in improving vegetation productivity historically and thus called OLMPs, can promote vegetation carbon sequestration once transferred/copied to neighboring locations with identical local conditions and lower $NPP_{CR}$, or the climate-rectified NPP (see "Methods"). Conversely,

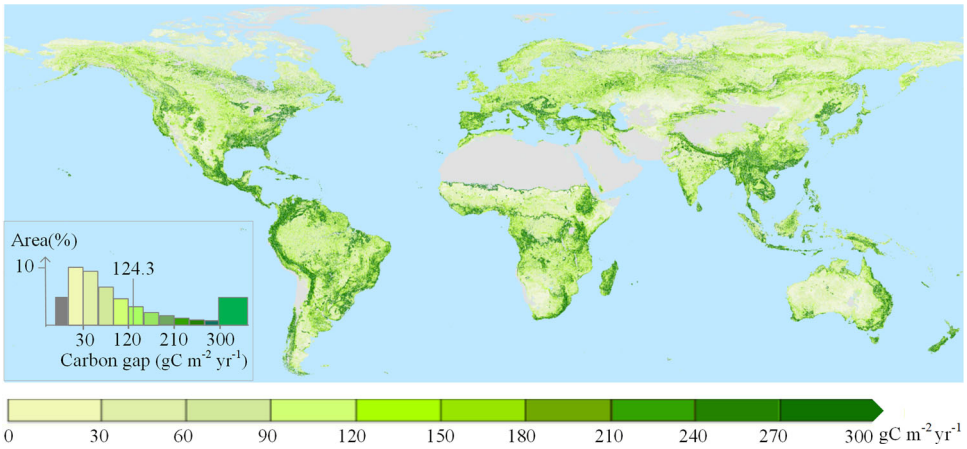


**Fig. 1 Distribution of global carbon gap density (flux).** The density is depicted through pixel values at 500 m × 500 m spatial resolution. The inset figure shows the histogram of area percentage in each of the bins of the carbon gap density. The most left gray bar indicates that these areas (=4.8% out of all vegetated areas which is $110.5 \times 10^6$ km$^2$) have carbon gap=0 (where $NPP_{CR} \geq NPP_{CR}^{90th}$), indicating LMPs already being OLMPs). The most right green bar, which also happens in about 4.8% of the total vegetated area, represents that those locations have the most highest carbon gap density (>300 gC m$^{-2}$ yr$^{-1}$). The vertical line in the inset histogram shows the location of the averaged carbon gap density (i.e., 124.3 gC m$^{-2}$ yr$^{-1}$) over the whole area of the 12 continents/regions (North America, Central America, South America, Europe, Africa, Australia, East Asia, North Asia, South Asia, Southeast Asia, Southwest Asia, and Central Asia). A total of more 13.74 PgC yr$^{-1}$ is expected to be sequestered from vegetation if OLMPs are implemented at a global scale.

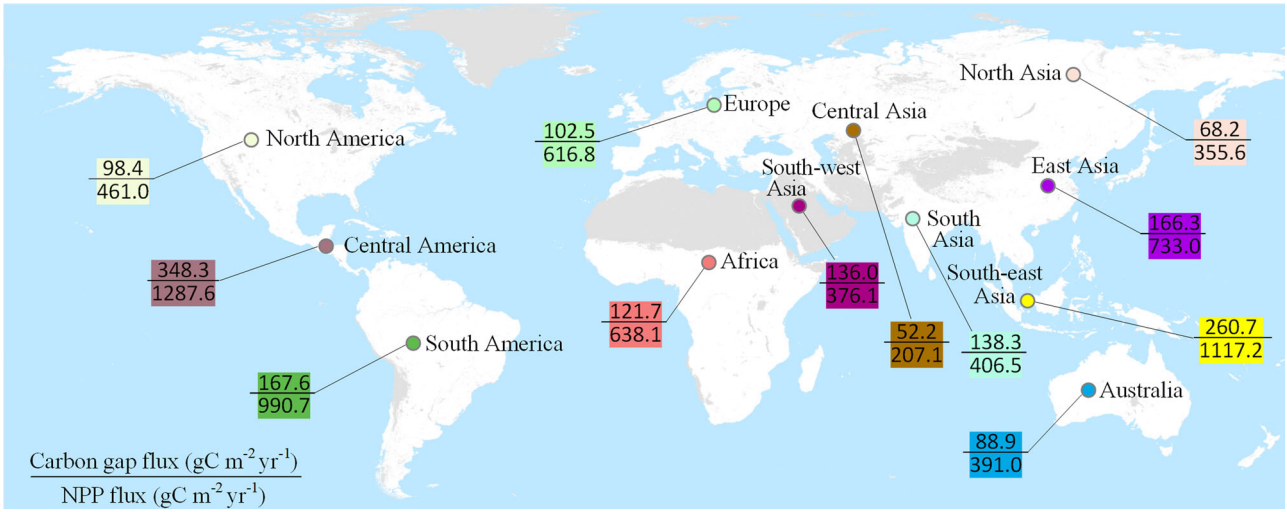


**Fig. 2 Carbon gap and NPP density averaged at continent (region) level.** The numerator and denominator of each fraction for the continents/regions show carbon gap flux/density (gC m$^{-2}$ yr$^{-1}$) and NPP flux (gC m$^{-2}$ yr$^{-1}$), respectively.

in grassland ecosystems where degraded vegetation showed decreased productivity due to overgrazing[27], measurements such as destocking rate or rotational grazing in a neighborhood could increase vegetation productivity[9,28]; thus, the practices of destocking and rotational grazing can be taken as OLMPs.

**The carbon gap differs among continents and biomes**. Considerable differences in the flux density of the carbon gap and NPP were observed among the 12 continents/regions (Fig. 2 vs. Supplementary Fig. 2). The total carbon gap and NPP of the continents/regions are summarized in Table 1. Central America and Southeast Asia present the highest carbon gap flux, reaching 348.3 and 260.7 gC m$^{-2}$ yr$^{-1}$, respectively; they can capture an extra portion of 0.17 and 1.11 PgC every year, respectively. Africa and North America have the largest vegetated area, and they can capture an extra 2.37 and 1.86 PgC yr$^{-1}$, respectively. South America ranks the third-largest in the vegetated area (i.e., 16.58 million km$^2$); because of its relatively high carbon gap flux which amounts to 167.6 gC m$^{-2}$ yr$^{-1}$, the carbon gap totals 2.78 PgC yr$^{-1}$, leading all the continents/regions. The total carbon gap is strongly correlated to the total NPP at the continental/regional level ($r = 0.98$) (Table 1). However, the carbon gap flux (density) is inconsistent with the NPP density at the pixel scale and within each continent/region. At the pixel level, the carbon gap flux and NPP flux are compared by the ratio, i.e., the carbon gap flux divided by the NPP flux at pixel basis, which clearly shows the high spatial variations (Supplementary Fig. 3). Furthermore, within each continent/region, the carbon gap density (Fig. 1) and NPP density (Supplementary Fig. 2) do not correlate well. This finding is confirmed by the scatter plots between the carbon gap density vs. NPP density (Supplementary Fig. 4) and notably illustrated by two typical rainforests, i.e., the Amazon rainforest located within South America and the African rainforests (Supplementary Fig. 5). Both the rainforests show highly dense NPP fluxes (1273.3 and 1062.7 gC m$^{-2}$ yr$^{-1}$ for Amazon and African

**Table 1 Statistical summary of the total carbon gap and NPP of the continents (regions).**

| Continent | Veg. area ($10^6 \times km^2$) | Carbon gap (std.) ($PgC\ yr^{-1}$) | NPP (std.) ($PgC\ yr^{-1}$) |
|---|---|---|---|
| Europe | 9.24 | 0.95 (0.05) | 5.7 (0.39) |
| Africa | 19.51 | 2.37 (0.13) | 12.45 (0.83) |
| Australia | 7.49 | 0.67 (0.05) | 2.93 (0.33) |
| East Asia | 11.66 | 1.94 (0.10) | 8.54 (0.42) |
| North Asia | 13.28 | 0.91 (0.06) | 4.72 (0.29) |
| South Asia | 4.03 | 0.56 (0.02) | 1.64 (0.09) |
| Southeast Asia | 4.26 | 1.11 (0.07) | 4.76 (0.25) |
| Southwest Asia | 1.93 | 0.26 (0.02) | 0.73 (0.06) |
| Central Asia | 3.18 | 0.17 (0.01) | 0.66 (0.09) |
| North America | 18.89 | 1.86 (0.17) | 8.71 (0.82) |
| Central America | 0.5 | 0.17 (0.01) | 0.64 (0.04) |
| South America | 16.58 | 2.78 (0.21) | 16.43 (1.31) |
| Total | 110.54 | 13.74 (0.78) | 67.90 (3.86) |

The total carbon gap and total NPP are both presented with averaged value ± standard deviation (std.) for each continent (region) over the years during 2001–2018 ($n = 19$). Note that the effect of reducing atmospheric $CO_2$ from the carbon gap is subject to vary due to soil heterotrophic respiration ($R_H$) which is estimated to be 0.71–0.74 (see "Methods"). The averaged carbon gap and averaged NPP for each continent/region are significantly correlated ($P < 0.01$, Pearson correlation coefficient $r = 0.98$).

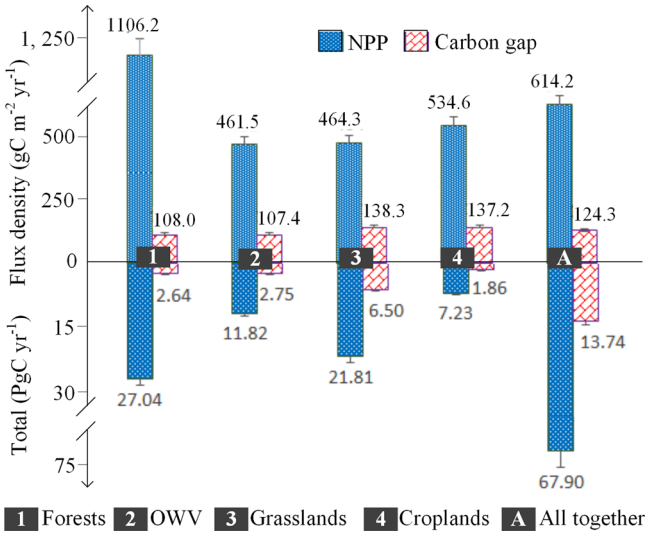


**Fig. 3 Comparison of the carbon gap and NPP across biomes.** The statistics summarize the carbon gap and NPP (total and flux) of the global vegetated area (see more on the definition of the vegetated area in Supplementary Table 3).

rainforests, respectively). These fluxes nearly double the globally averaged NPP flux (614.2 $gC\ m^{-2}\ yr^{-1}$); however, their carbon gap flux averages 117.5 and 121.1 $gC\ m^{-2}\ yr^{-1}$, respectively, at a comparable level to that of the continentally averaged level, i.e., 124.3 $gC\ m^{-2}\ yr^{-1}$. The carbon gap varies among different biomes (see definition in Supplementary Table 3 and Supplementary Fig. 6). Grasslands and croplands disclose the maximum carbon gap density, reaching 138.3 and 137.2 $gC\ m^{-2}\ yr^{-1}$, respectively (Fig. 3). Forests show somewhat limited potential in the carbon gap, only 107.99 $gC\ m^{-2}\ yr^{-1}$ in the flux and 2.64 $PgC\ yr^{-1}$ in the total, though the forests NPP flux almost doubles the global averaged (1106.2 $gC\ m^{-2}\ yr^{-1}$ vs. 614.2 $gC\ m^{-2}\ yr^{-1}$). The total NPP of forests is more than 1/3 of all other vegetation types together (i.e., 27.04 $PgC\ yr^{-1}$ vs. 67.9 $PgC\ yr^{-1}$) (Fig. 3 and Supplementary Fig. 7). The other woody vegetation (OWV), though presenting

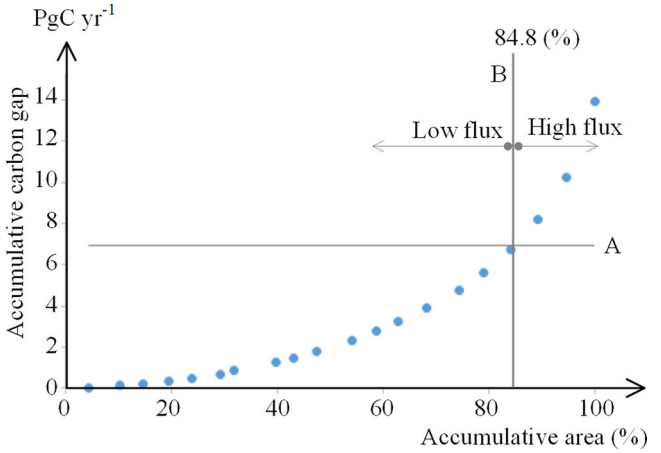


**Fig. 4 Accumulative total carbon gap against the accumulative total vegetated area.** The whole vegetated area is first sliced into sub-areas using the percentiles of carbon gap flux (from low to high) at an interval of 5%, i.e., 0~5%, 5~10%, ..., and 95~100%. The accumulated area in the order of the percentiles is depicted on the *X* axis. The corresponding accumulated total carbon gap is shown on the *Y* axis. The horizontal line (A) shows the location of half (50%) of the accumulative total carbon gap. The vertical line (B) denotes the location of the separator that divides the accumulated areas into two equal parts (low flux side and high flux side), where both sides collect half (50%) of the total carbon gap. While representing only ~15% of the total area, the high flux side collects half of the total carbon gap.

much lower NPP flux and total NPP, shows a carbon gap flux and total carbon gap comparable to those of forests, which are 107.4 $gC\ m^{-2}\ yr^{-1}$ and 2.75 $PgC\ yr^{-1}$, respectively. Because grasslands cover the largest area (46.97 million $km^2$, Supplementary Table 4) and present the highest carbon gap flux, i.e., 138.3 $gC\ m^{-2}\ yr^{-1}$, the total carbon gap accounts for nearly half of the all summed total, reaching 6.5 $PgC\ yr^{-1}$. Croplands can sink atmospheric $CO_2$ with the adoption of improved context-specific land management[29]. Croplands show relatively high carbon gap flux, 137.2 $gC\ m^{-2}\ yr^{-1}$. However, croplands cover the least land area (13.52 million $km^2$), making the total carbon gap the lowest, i.e., 1.86 $PgC\ yr^{-1}$ only.

The carbon gap flux presents a strong clustering pattern, which is reflected by the comparison between the accumulative carbon gap and the accumulative sliced vegetated area using the carbon gap flux from low to high (Fig. 4 and Supplementary Fig. 8). On average, ~50% of the total carbon gap comes from only ~15% of the global vegetated area. In terms of OLMP implementation, the finding suggests that only a small part of the prioritized vegetated area, i.e., ~15% of total vegetated coverage, would add more 6.87 $PgC\ yr^{-1}$ (i.e., 50% of the total carbon gap) in vegetation productivity.

**Human activities strongly affect the carbon gap**. We examine the relationship between the carbon gap and the population, as human density is a good indicator of human activities[30]. The world population varies substantially over the space between continents/regions (Fig. 5 and Supplementary Table 5). South Asia, East Asia, and Southeast Asia present the most densified population, followed by moderately populated Southwest Asia, Europe, and Africa. At the global level, there exists no close link between the carbon gap flux and population density (Pearson's correlation coefficient $r = 0.27$; see Supplementary Table 5). However, they demonstrate strong correlations at the continental/regional scale. The β coefficients of their regression lines are

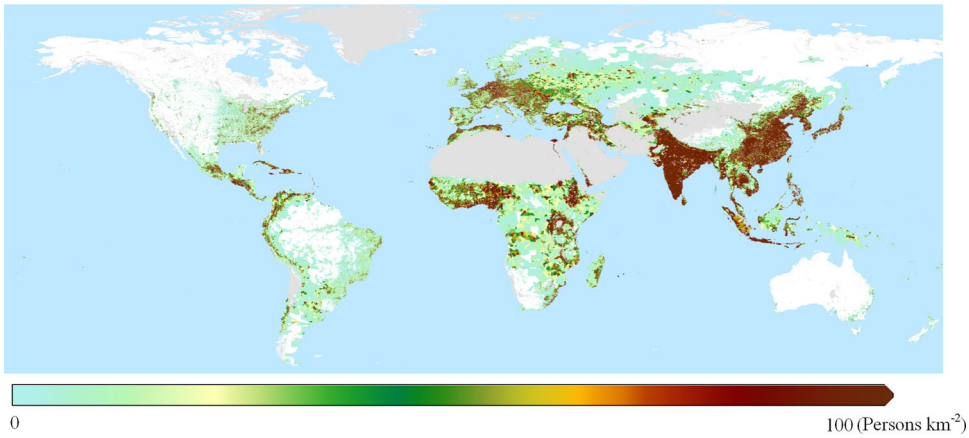


**Fig. 5 Distribution of world population density.** Gray background is non-vegetated (see biomes definition in Supplementary Table 3) that is excluded from analysis and white areas show population density 0.

**Table 2 Regression between carbon gap flux and population density.**

| Continent | Slope (β) | *t*-value[a] | −95%[b] | +95%[c] | $R^2$ |
|---|---|---|---|---|---|
| Europe | 12.48 | 9.48* | 9.71 | 15.24 | 0.83* |
| Africa | 11.29 | 9.95* | 8.82 | 13.76 | 0.89* |
| Australia | 79.92 | 15.14* | 68.16 | 91.68 | 0.96* |
| East Asia | 6.53 | 6.80* | 4.47 | 8.59 | 0.77* |
| North Asia | 145.76 | 8.96* | 110.86 | 180.66 | 0.85* |
| South Asia | 2.69 | 4.23* | 1.31 | 4.06 | 0.59* |
| Southeast Asia | 5.14 | 3.75* | 2.23 | 8.05 | 0.47* |
| Southwest Asia | 11.49 | 3.48* | 4.56 | 18.42 | 0.40* |
| Central Asia | 12.51 | 11.54* | 10.21 | 14.81 | 0.89* |
| North America | 20.78 | 36.28* | 19.54 | 22.06 | 0.99* |
| Central America | 14.16 | 4.17* | 7.01 | 21.28 | 0.49* |
| South America | 28.16 | 10.02* | 22.16 | 34.15 | 0.87* |

*Significance level = 0.01, [a] the *t*-value for the slope (β), showing significant ($P < 0.01$) and positive (slope > 0) for all the continents/regions, [b]95% lower, and [c]95% upper bound for the slope.

positive and statistically significant over all the continents (Table 2 and Supplementary Fig. 9). The goodness of fit of the regression models ($R^2$) differs probably due to the varied spatial configuration in population distribution and biophysical environments reflected by LVS factors. The findings suggest that the areas with intensive human influences are more likely to note high carbon gap flux, primarily observed in densely populated areas (Figs. 1 and 5). At the same time, the impact on the carbon gap from human activities is not independent of the biomes distribution, which is noticeably observed in the plain region of Eastern China and some plain regions of India presenting the most densely populated but relatively lower carbon gap flux (Figs. 1 and 5). Those plain regions show relatively low NPP flux (Fig. 5 and Supplementary Fig. 2), and thus the carbon gap density will also be low (see "Methods"). One explanation is that these plain regions have long been cultivated. These regions' crop production management practices are well optimized and fit their environments. In other words, these regions have realized OLMPs to some extent. Therefore, the NPP variability is very limited in these regions. As a case of human activities, updating LMPs can alter vegetation NPP in terrestrial ecosystems, either positively or negatively[22,28]. The study verifies that human activities have generally increased the carbon gap in the past two decades and thereby, policy interference should focus more on those highly populated areas.

## Discussion

The Paris Climate Agreement proposed national contributions to the goal of holding global warming to well below 2 °C[3]. Assessing the carbon gap, i.e., how much more carbon is to be sequestered through optimal land-management practices (OLMPs), is helpful to mitigate climate changes. This study combines time-series remote sensing datasets, partitioned landscape–vegetation–soil (LVS) zones, and distance-constrained zonal analysis to identify OLMPs and assess the carbon gap (see "Methods"). We estimate that ~1/5 more carbon, totaling 13.74 PgC $yr^{-1}$, could be added to the current NPP from global terrestrial vegetation if the identified OLMPs get implemented, or a net effect of reducing 3.5–4.0 PgC $yr^{-1}$ from the atmosphere. On average, the carbon gap flux is 124.3 gC $m^{-2}$ $yr^{-1}$, with large variations among the continents/regions and the vegetation biomes. Central America and Southeast Asia present the highest carbon gap flux, reaching 348.3 and 260.7 gC $m^{-2}$ $yr^{-1}$, respectively. Grasslands show the most potential in improving carbon sequestration, with a carbon gap flux of 138.3 gC $m^{-2}$ $yr^{-1}$ and a total carbon gap of 6.5 PgC $yr^{-1}$. Half of the total carbon gap concentrates in ~15% of the vegetated area, where particular policy-making attention needs to focus. In other words, location-dependent OLMPs should be prioritized to fill the carbon gaps, particularly in the ~15% areas with the highest potential.

Improving land-management actions can add to nationally determined contributions (NDCs) to the Paris Agreement[31,32]. Previously, it was reported that land use, land-use change, and forest (LULUCF) sector could contribute to as much as 20% of the mitigation potential of NDC targets at the global level[33]. Our study suggests the contributions from LULUCF to NDC targets might be greatly underestimated, as applying OLMPs alone can reduce more than 1/3 of the current global fossil fuel emissions. The net atmospheric carbon reduction from OLMPs varies among countries/regions, including China, USA, the EU28, and India, which have the most fossil carbon emissions or/and the largest population (Supplementary Table 6)[4]. As the largest population in the world, China emits the most total greenhouse gases in recent years[4]. China has declared to realize the peaking of carbon emissions around 2030 in its NDC under the Paris Agreement. Successfully fulfilling the NDC targets depends on substantial efforts to fully implement all current policies and adopt more effective policies after 2020[34]. Implementing OLMPs could account for 11–12% of its current carbon emissions, which can play an important role in achieving the NDC target of the country. USA is one of the most developed countries having the second-largest carbon emission and has promised to achieve

26–28% emission reductions below the 2005 level in 2025 in its first NDC and 50–52% reductions in 2030 in the second. Implementation of OLMPs in USA will contribute 27–31% carbon emission reduction. As the world's biggest economy and the third biggest carbon emitter, the EU28 recently set its NDC target to a net decrease in emissions by 55% from the 1990 level by 2030[35]. The carbon gap through implementing OLMPs could contribute 28–31% reduction of the EU28's fossil carbon emissions, compensating more than half of its NDC target. India is the world's second-largest populated country which emitted 0.74 PgC in 2018. The NDC target from India pledges 33–35% reduction in the emissions intensity of its GDP from the 2005 level by 2030[36]. Implementation of OLMPs can help India neutralize 15–16% carbon emissions at the level of 2018.

The varied carbon gap among different biomes provides essential information for designing OLMP implementation strategy. The higher carbon gap fluxes in grasslands and croplands indicate that they have a quicker or more sensitive response to human activities (i.e., updated LMPs) than the forests and OWV. For grasslands and croplands, vegetation productivity improvement (or degradation) may take a shorter period to appear (e.g., within a calendar year) once LMPs are updated. Conversely, apart from abrupt intervention from human activities such as massive reforestation or deforestation[9], forests and OWV vegetation may take a relatively longer time to show up the effect from updated LMPs. Thus, grasslands and croplands have the advantage of showing immediate benefit, i.e., increased carbon sequestration, from the implementation of OLMPs. On the other hand, it requires a long-term plan to improve carbon sequestration for forest and OWV ecosystems.

OLMPs correspond to one or a set of LMPs that have historically proved to be able to produce higher $NPP_{CR}$ (≥90th percentile of $NPP_{CR}$) at locations within an environmentally (climatically and non-climatically) homogeneous neighborhood. In the farm-dominated regions, LMPs such as cropping rotation, farm irrigation, or compost amendments effectively improved agriculture productivity[9]. Multiple cropping, fertilizer application, and irrigation in China and India's agricultural lands had contributed to the greening Earth as a result of an observed increase in green leaf area[37]. Cover crops are commonly included in strategies aimed at increasing agricultural production[38]. Planting cover crops play an important role in improving the productivity of subsequent crops[39]. Reforestation, or planting trees in areas that have been degraded or deforested, can promote restoration of forest structure and vegetation productivity by regrowing tree canopy and preserving biodiversity, thus improve carbon sequestration[40]. The previous study suggests that land-cover transformation from one type to another, e.g., afforestation from croplands, can sequester more carbon[22]. However, while afforestation has been suggested for degraded croplands[22,23], concerns arise from decreased food supply due to a reduction in croplands resulting from afforestation. Hence, improving carbon sequestration through land conversions is not widely acceptable. Instead, it achieves more ecological and social benefits to obtain the carbon gap by tailoring land-management practices (i.e., by adopting OLMPs) without changing land use or land-cover types. Moreover, the referenced OLMPs are located within a neighborhood of ~20 km, which provides convenience for field verification and result evaluation in OLMPs implementation.

Nevertheless, there are a few concerns that may cause uncertainties, requiring further improvement and exploration. First, the referenced target NPP, i.e., $NPP_{CR}^{90th}$, could come from optimal LMPs that induce extra GHGs emissions, e.g., $N_2O$ (for instance, fertilizer application in croplands). As a result, the net effect of mitigating GHGs through OLMPs in some areas could be overestimated. Conversely, because the GHGs mitigation is estimated based on historical LMPs, it is unrealistic to identify OLMPs that are not historically present, meaning that the estimated carbon gap is likely to be underestimated due to the lack of referenceable OLMPs. Second, while land-management optimization can achieve higher NPP (and vegetation carbon sequestration), an implementation of OLMPs for ecological benefits (i.e., more NPP and carbon sequestration) may contradict other socioeconomic needs e.g., maximizing the production of grains or other edible produces. Furthermore, implementing OLMPs could involve extra input (e.g., labor or other resources), offsetting the willingness to implement the OLMPs widely. Under those cases, the land-management optimization could be adjusted to a lower target potential NPP, e.g., from the current 90th percentile ($NPP_{CR}^{90th}$) to the 80th percentile, which will allow more candidates of OLMPs for options. Third, the relative contribution (RC, see definition in Eq. (2)) on NPP due to the climate variations could be biased. The assumption that the contribution from HUMAN impact is reflected in the spatial variation of the climate-rectified NPP ($NPP_{CR}$) by subtracting RC from NPP in LVS zones, as shown in Eq. (3), may not hold due to possible interaction effect between the climate and HUMAN impact. Furthermore, though the Miami model provided a good approximation of the global distribution of potential vegetation productivity[41], it is empirically based, which could produce a biased estimate of RC of the climate variations by Eqs. (1) and (2). Improved methods capable of modeling the relative contribution of climate variations in LVS zones are undoubtedly helpful for a more accurate estimate of the carbon gap. Lastly, while the landscape–vegetation–soil (LVS)-based segmentation is designed to create biophysically homogeneous zones as the most important biophysical units for assessing carbon gap, the LVS segmented zones may not be internally homogeneous due to possible noises in the landforms (L), vegetation (V) cover, and soil (S) datasets. Notably, in areas such as mountainous regions (e.g., Himalayas and Andes), which are characterized by complicated landscapes, the relatively coarse spatial scale (500 m) of the datasets adopted in this study may not be able to capture the biophysical heterogeneity within an LVS zone. Such heterogeneity not expected in an LVS zone due to the lack of high-quality datasets at a global scale means more diversity in environmental conditions, resulting in higher NPP variability and higher $NPP_{CR}$ variability in the LVS zone. Thus, compared to many plain regions across the global terrestrial ecosystems, areas with complicated landscapes are more likely to present an overestimated carbon gap. In addition, some other complex factors, such as seasonal hydrologic pulsing[42] and nitrogen deposition[43], may affect vegetation productivity but were not included in the current design. As a result, the spatial variability in the biophysical environments related to NPP might not have been fully addressed by the LVS segmentation. Furthermore, wetlands were excluded in the analysis in the carbon gap. Vegetation in wetland ecosystems is sensitive to water depth variations (particularly in complex terrains close to water bodies and lakes)[44], hydrologic alterations[42], sediment and turbidity[45], and even transferred pollutant elements[46]. The impacts of these hydrological processes on NPP are challenging to model at a global scale. Considering that wetlands cover only about ~1% of the total land area (see Supplementary Table 3), excluding wetlands should only have a limited impact on the globally estimated carbon gap patterns. Because the detailed biophysical and socioeconomic datasets (including LMPs) are rarely available at a global scope, the uncertainties raised from the lack of high-quality datasets are challenging to address in this work. We suggest that refined assessment of enhancing vegetation productivity through OLMPs be conducted at a national scale with the support of detailed socioeconomic contextual datasets and biophysical datasets for

different terrestrial ecosystems. Nevertheless, the potential of improving carbon sequestration through OLMPs is confirmed, though designing practicable schemas for OLMPs implementation requires multiple participations from both governments and private sectors to work together.

## Methods

We divide the factors affecting vegetation carbon sequestration into three categories[16]:

1. Climate impact (typically precipitation and temperature)
2. Other nonclimatic environmental/natural factors, including landforms (L), vegetation (V) types, and soil (S) property
3. Human-related land-management practices (HUMAN)

Once the differed impact on vegetation carbon sequestration from the climatic (1) and nonclimatic (2) is excluded, the difference in the carbon sequestration from vegetation over space will be solely attributed to site-specific HUMAN (3) impact. We apply net primary productivity (NPP) to indicate the capacity of vegetation carbon sequestration in terrestrial ecosystems. The method is developed based on the following assumptions:

- NPP is jointly affected by (1) climate impact, (2) LVS (landscape–vegetation–soil) environmental or biophysical factors, and (3) HUMAN activities (land-management practices, LMPs).
- Over a homogeneous LVS segmented zone, the climate factors and HUMAN factors are the most important ones explaining the NPP variation in an LVS zone. The climate's potential impact on vegetation productivity in an LVS zone can be indicated by climate-driven NPP models such as Miami, called potential NPP (PNPP).
- The variation of NPP from the differed climate factors in an LVS zone can be measured by a statistic called Relative Contribution (RC) of the climate factors. RC is the difference between PNPP at a location in an LVS zone and the averaged PNPP of the whole zone.
- RC is designed to rectify the relative impact of the climate factors on NPP over an LVS zone to derive climate-rectified NPP, or termed as $NPP_{CR}$. The variation of $NPP_{CR}$ over the LVS zone is then attributed to HUMAN influence.

Our main objective is to assess how much more carbon (termed as carbon gap) can be realistically achieved from global terrestrial vegetation by updating HUMAN only, without converting land use and land cover or vegetation biomes. We use publicly available time-series of datasets to analyze the carbon gap. Data sources come from Google Earth Engine (GEE). Data preprocessing and analysis are also performed on the GEE computing platform. There are four groups of data sources involved, namely climate-related variables, (non-climate) physical environmental variables, NPP, and world population. Those datasets, if not at the scale of 500 m, are uniformly be resampled to a resolution at 500 m. The following explains the steps of data processing and analysis methods.

**Region segmentation of homogeneous natural environments to detach non-climate impacts on NPP variation**. Region segmentation is performed by overlaying the layers of landform (L), vegetation type (V), and soil type (S) to derive homogeneous zones, known as homogeneous LVS zones so that all locations (image pixels) in an LVS zone will have the same LVS# of landform, vegetation, and soil type. In other words, over the pixels within the same LVS zone, the impact from the non-climate environmental factors on the internal NPP variation is uniform. Thus, any NPP variation within an LVS zone is attributed to varied climatic and HUMAN impacts only.

The three environmental factors, namely landforms, biomes types, and soil profiles, are chosen for LVS segmentation because of the following considerations. First, landform properties are often used to represent the spatial variability of hydrological, geomorphologic, and biological processes[47]. Here, we use the classified landform cover from European Soil Data Centre (https://esdac.jrc.ec.europa.eu) to indicate landform variations. This landform cover includes 16 labels dynamically classified by an unsupervised nested-means algorithm based on three geometric criteria (slope, surface texture, and local convexity) from the Shuttle Radar Topography Mission 30 m (SRTM30) digital elevation data[48]. Second, the International Geosphere-Biosphere Programme (IGBP) land-cover classification schema of MODIS MOD12Q1 (asset ID=MODIS/006/MCD12Q1 in GEE) is taken to map vegetation (biome) distributions. According to the IGBP land-cover classification system, there are 17 labels, out of which 13 are closely related to vegetation cover types. Five of them (13# urban and built-up lands, 15# snow and ice, 16# barren, 17# water bodies, and 11# permanent wetlands) are excluded from further analysis (Supplementary Fig. 6 and Supplementary Table 3). Wetlands have been shown to play an important role in global carbon exchange[49]. However, our exploratory analysis reveals that spatial variation of NPP in wetlands in most areas is huge, which we believe could not be explained simply by the biophysical environment differences indicated by LVS factors. We attribute the large NPP variation in wetlands to other factors such as variations in water depth (in complex terrains close to water bodies and lakes)[44], hydrologic alterations[42], sediment, and turbidity[45], and even variations in pollutant elements transferred through water movement[46]. Furthermore, the wetlands area covers only about ~1% of the total land area (see Supplementary Table 3). Excluding wetlands should have a limited impact on the globally estimated carbon gap. Thus, only 12 land-cover classes were analyzed for sinking $CO_2$ from the atmosphere in this study. Lastly, Harmonized World Soil Database (HWSD, ver. 1.2 from Food and Agriculture Organization, http://www.fao.org/soils-portal) is the most up-to-date world soil map that incorporates a data table of 48,148 soil profile descriptions related to the various soils associated with each mapping unit, at a spatial resolution 1 km at the equator[50]. Thus, soil-type classes from FAO-90 code (SU_Code90), which includes 194 labels, are used for mapping soil-type cover.

**Rectifying the climatic impact on NPP**. NPP dataset provides a direct indicator of carbon sequestration from vegetation. The MODIS MOD17A2H product (V6) is a cumulative 8-day composite at 500-m spatial resolution. MOD17A2H includes a layer of net photosynthesis, an indicator of NPP reflecting the spatiotemporal variations in vegetation carbon sequestration.

In terms of the climatic factors, precipitation and temperature are the most important elements because both of them were confirmed to alter NPP and thus carbon uptake from vegetation[51]. Theoretical NPP has been modeled purely from climatic conditions; the climate-driven empirical Miami model is considered the first to compute PNPP using monthly precipitation and temperature and is often used as a baseline for model comparison[52]. The modeled PNPP exhibits many spatial variations, reflecting spatial heterogeneity of the impact of the climatic factors.

We assume that the Miami model can be applied to measure the relative impact on NPP from climate variations in an LVS zone. The Miami model is used to assess the climate impact on PNPP, which takes the form[51],

$$\mathrm{PNPP} = \lambda \times \min\left\{\frac{3,000}{1+e^{1.315-0.119t}},\ 3,000\times\left(1-e^{-0.000664p}\right)\right\} \quad (1)$$

where $t$ is the annual average temperature (°C), $p$ is the annual precipitation (mm), and $\lambda$ is a conversion coefficient (0.50 for woody ecosystems and 0.45 for herbaceous) that converts dry matter to carbon unit ($gC\,m^{-2}\,yr^{-1}$). TerraClimate derived from climatically aided interpolation by combining WorldClim dataset and Climatic Research Unit Time-Series dataset has been widely applied for mapping regional and global ecological parameters[53]. It provides monthly precipitation and maximum/minimum temperature at the spatial resolution of 2.5 arc minutes. Equation (1) describes the relationship between PNPP and two climatic variables, $p$ and $t$.

For discriminating the varied climate impact on NPP in an LVS zone, a location-dependent relative contribution (RC) of climate factor is defined as the difference between PNPP at location $i$ in an LVS zone $g$ and the averaged PNPP of the whole $g$, namely,

$$\mathrm{RC}(i,g) = \mathrm{PNPP}(i,g) - \mathrm{PNPP}_{\mathrm{Mean}}(g) \quad (2)$$

where PNPP($i$,$g$) is PNPP at $i$ in $g$, $\mathrm{PNPP}_{\mathrm{Mean}}(g)$ is the mean PNPP of all the locations in $g$, namely $\mathrm{PNPP}_{\mathrm{Mean}}(g) = \sum_{i=1}^{n_g}\mathrm{PNPP}(i,g)/n_g$ and $n_g$ is the total number of locations (pixels) in $g$. RC($i$, $g$) is the difference between PNPP at $i$ and $\mathrm{PNPP}_{\mathrm{Mean}}(g)$ due to within-group variation of the climate impact. Clearly, $\sum_{i=1}^{n_g}\mathrm{RC}(i,g) = 0$. The rationale is that more favorable climate conditions at a location $i$ will result in a positive and higher RC($i$,$g$) and vice versa.

The climatic and HUMAN impact determine the NPP variations across an LVS zone characterized by the identical landform, vegetation cover, and soil properties. The assumption is that the climatic impact on NPP variations can be estimated by RC on a location basis in an LVS zone. Climate-rectified NPP ($NPP_{CR}$) at location $i$ in $g$ can be derived using the function,

$$\mathrm{NPP}_{\mathrm{CR}}(i,g) = \mathrm{NPP}(i,g) - \mathrm{RC}(i,g) \quad (3)$$

$NPP_{CR}$($i$,$g$) is the rectified NPP at location $i$ in $g$ after the climatic impact on NPP is removed by applying Eq. (3). Considering $\sum_{i=1}^{n_g}\mathrm{RC}(i,g) = 0$, it is clear that $\sum_{i=1}^{n_g}\mathrm{NPP}_{\mathrm{CR}}(i,g) = \sum_{i=1}^{n_g}\mathrm{NPP}(i,g)$. In other words, the NPP distributions over $g$ are readjusted to $NPP_{CR}$ by taking the zonal climate variations into account through Eq. (3). The internal variation of the computed $NPP_{CR}$ across all the locations in the LVS zone $g$ will then be attributed to HUMAN impact only. Thus, after the climate rectification, $NPP_{CR}$ should be free of variations of the effect of climate factors in each LVS zone. $NPP_{CR}$ would assume a constant value if there were no differed HUMAN impacts within an LVS zone. When spatial variations of $NPP_{CR}$ within an LVS zone are observed, it is attributed to HUMAN influence, i.e., the difference in land-management practices (LMPs). Those locations showing low $NPP_{CR}$ are not managed well from the perspective of their current carbon sequestration. Particularly, for locations with negative $NPP_{CR}$ ($NPP_{CR} < 0$), the HUMAN impact on NPP is negative. Thus, carbon gaps over these locations are considerable. On the contrary, the locations (pixels) showing relatively very high $NPP_{CR}$ values can be regarded where good LMPs are practicing. These good LMPs can be deemed to be the optimal LMPs (OLMPs) under similar environmental conditions over this LVS zone. The varied $NPP_{CR}$ in an LVS zone suggests that introducing the LMPs in the current LVS zone can sequester more carbon. In other

words, through human policy and management interventions, the LMPs at locations (pixels) with lower $NPP_{CR}$ in the LVS zone could be replaced by the OLMPs at places with higher $NPP_{CR}$ to increase carbon sequestration to a higher level.

**Computing carbon gap by distance-constrained (DC) zonal analysis**. The OLMPs and carbon gaps are processed for each location. The carbon gap at a given location is computed as the gap from its current $NPP_{CR}$ to a target NPP level that is the most achievable high $NPP_{CR}$ at locations with identical or similar environmental contexts (i.e., in the same LVS zone). We develop a distance-constrained zonal analysis to evaluate the target NPP level. Zonal analysis computes a set of statistics (e.g., maximum, median, or minimum value) from the input values of $NPP_{CR}$ within a zone[54]. The maximum zonal $NPP_{CR}$ ($NPP_{CR}^{Max}$) is the highest $NPP_{CR}$ corresponding to the best land-management practice (BLMP) in the zone; if BLMP is adopted, it will present the highest carbon gap. However, a zonal statistic defined as the 90$^{th}$ percentile, or $NPP_{CR}^{90th}$, from the input vector of $NPP_{CR}$ is selected as the referenced target NPP level in this study. The selection of $NPP_{CR}^{90th}$ instead of $NPP_{CR}^{Max}$ in an LVS zone can exclude exceptionally high $NPP_{CR}$ values, which are likely outliers resulting from noisy data, or are hardly achievable by other locations even in the same LVS zone. Thus, the zonal statistic $NPP_{CR}^{90th}$ provides a more robust reference as the target potential NPP level. The LMPs at locations showing $NPP_{CR} \geq NPP_{CR}^{90th}$ will be referenced as the OLMPs for other locations in a similar environmental context.

The appraisal of the $NPP_{CR}^{90th}$ at a location is conducted among locations labeled as the same LVS# within a local neighborhood. It is argued that the variations of $NPP_{CR}$ at locations within an LVS zone are attributed to the differences in HUMAN impacts (i.e., LMPs). It is also acknowledged that other omitted factors may impose an unneglectable impact on vegetation carbon sequestration, which could produce certain uncertainties in the isolation of HUMAN impact. Thus, the determination of OLMPs is preferably performed at local scope. In other words, LMPs at locations too far away from the currently examined location could be affected by too many heterogeneous economic, social, and political factors. Furthermore, locally referenced OLMPs are more practical for policy implementation and make it possible for on-site checkout.

A window size specifies a local neighborhood surrounding given location *i*, in which the $NPP_{CR}$ values at all the locations with the identical LVS# in this window are taken as input to compute the $NPP_{CR}^{90th}$. To decide the window size, a stratified random selection approach is taken to sample 5000 points in the vegetated land with the sample size weighted by the area of each of the biome types. The samples' histogram shows peak $NPP_{CR}^{90th}$ along with the distance, which presents a relatively stable stage when the distance is over 20 km from the piecewise linear function fitting (Supplementary Fig. 1). Hence, the carbon gap at location *i* is computed as the difference between the current $NPP_{CR}$ and the $NPP_{CR}^{90th}$ within the 20 km window in the environmentally homogeneous zone (i.e., LVS zone).

$$\text{Carbon gap}_i = \max(0, NPP_{CR}^{90th} - NPP_{CR}^{i}) \quad (4)$$

where $NPP_{CR}^{90th}$ corresponds to the statistic of the 90th percentile for $NPP_{CR}$ input at all locations labeled as the same LVS# in the distance-constrained neighborhood, $NPP_{CR}^{i}$ is $NPP_{CR}$ for location *i*, and max is the function for getting the maximum value from the two input 0 and $NPP_{CR}^{90th} - NPP_{CR}^{i}$, meaning that if the $NPP_{CR}$ at the location *i* is less than the $NPP_{CR}^{90th}$, the carbon gap will be equivalent to $NPP_{CR}^{90th}$ minus $NPP_{CR}^{i}$; otherwise, the land-management practice (LMP) at location *i* has already reached the level of carbon sequestration under OLMP and no extra space of carbon sequestration is available (i.e., carbon $gap_i = 0$, if $NPP_{CR}^{i} \geq NPP_{CR}^{90th}$). The carbon gap is not only dependent on the $NPP_{CR}$ variability but also constrained by the level of $NPP_{CR}$. It is reasonable that areas with a low NPP (and accordingly $NPP_{CR}$) density cannot be expected to have a higher carbon gap density. Note that low NPP values in non-vegetated areas (corresponding to the IGBP land-cover types labeled as 13# urban and built-up lands, 15# snow and ice, 16# barren, 17# water bodies) which have been previously excluded are not used in the $NPP_{CR}^{90th}$ computation. Thus, the candidate of OLMPs for a location is decided by referring to the LMPs within the distance-constrained local window that boast identical environmental contexts but exhibit a higher level of carbon sequestration (i.e., where $NPP_{CR} \geq NPP_{CR}^{90th}$).

The carbon gap flux and NPP flux are shown in Fig. 1 and Supplementary Fig. 2. The annual changes in the carbon gap and NPP are summarized in Supplementary Table 4. The ratio map of carbon gap density to NPP density is shown in Supplementary Fig. 3. The carbon gap and NPP (total and flux density, respectively) among the biomes and continents/regions are compared in Supplementary Fig. 7.

**Effect of reducing atmospheric $CO_2$ from the carbon gap**. The resultant carbon gap suggests an increase of NPP 13.74 PgC yr$^{-1}$ with OLMPs implemented (Supplementary Table 2). When considering the possible increase in soil heterotrophic respiration ($R_H$), the improved NPP's net effect (i.e., the carbon gap) on reducing atmospheric $CO_2$ is less than this total NPP. Previous studies show that the total amount of $R_H$ is mainly proportional to NPP; for example, the previous study showed that the ratio of $R_H$ to NPP was 0.71[13]. A meta-analysis on $R_H$ from the available dataset estimated that the global weighted mean $R_H$ was 457 ± 139 gC m$^{-2}$ yr$^{-1}$ [55]. Our study indicates that the average NPP over the study years is 614 ± 35 gC m$^{-2}$ yr$^{-1}$ (Supplementary Table 2), suggesting that the ratio of $R_H$ to NPP is 0.74 (=457/614), which is reasonably close to the previous study[13]. Taking the ratio of $R_H$ to NPP between 0.71 and 0.74 (though the ratio is subject to vary on a broader scope under climate changes), an increase of NPP (the total carbon gap) 13.74 PgC yr$^{-1}$ is estimated to reduce 3.5–4.0 PgC yr$^{-1}$ from the atmosphere.

**Correlation analysis between total carbon gap and total NPP**. The relationship between the total carbon gap and total NPP at the global scale is revealed by Pearson's correlation analysis on the two variables, i.e., total carbon gap and total NPP for each continent/region, resulting in Pearson correlation coefficient $r = 0.98$ (Fig. 2). The relationship between the carbon gap flux and NPP flux at the sub-continental/regional level is performed by slicing the carbon gap density into partitions based on the ordered percentiles of the carbon gap flux (from low to high) at an interval of 5%, i.e., 0–5%, 5–10%, …, and 95–100% for each continent/region (Supplementary Fig. 4). Comparison between the total carbon gap and total NPP for two typical regions, i.e., amazon rainforests and the rainforests of Africa, is further illustrated in Supplementary Fig. 5.

**Analyzing the distribution pattern of the carbon gap**. For each of the 12 continents/regions, the carbon gap flux is grouped based on the sliced percentiles (from low to high) at an interval step of 5%, i.e., 0–5%, 5–10%, …, and 95–100%. The vegetated area and total carbon gap within each percentile are then computed. The points denoted by the accumulative vegetated area and the accumulative total carbon gap in each percentile are used to reveal the carbon gap's clustering pattern (Supplementary Fig. 8). The maximum accumulative total carbon gap is divided into two half-half sections by a horizontal line, i.e., low flux density and high flux density. The global clustering pattern in the carbon gap distribution is similarly derived (Fig. 4).

**Regression analysis between carbon gap and population density**. For each of the 12 continents/regions, the carbon gap density is grouped based on the sliced percentiles (from low to high) at an interval step of 5%, i.e., 0–5%, 5–10%, …, and 95–100%. We then compute the accumulative total carbon gap and accumulative total population. The relationships between the accumulative total population and the accumulative total carbon gap are graphed by the sliced percentiles. Linear regressions are fit for the partitions with the accumulative total carbon gap set as the dependent variable and the accumulative total population for each percentile as the independent variable (Table 2 and Supplementary Fig. 9).

The world population data comes from the Gridded Population of World (Ver. 4, from NASA Socioeconomic Data and Applications Center)[56], which models the distribution of the global human population for the years 2000, 2005, 2010, 2015, and 2020 on 30 arc-second grid cells. A proportional allocation gridding algorithm, utilizing millions of national and sub-national administrative units, is used to assign population counts to 30 arc-second grid cells. The averaged population density and carbon gap flux within each continent/regions is summarized in Supplementary Table 5.

**Validation of the estimated carbon gap**. Systematic validation of the estimated carbon gap is challenging because it requires long-term field experiments for different ecosystems and biomes across the globe. We test the result of the carbon gap on the typical grassland in the Inner Mongolia Autonomous Region (IMAR) in China based on long-term field monitoring of vegetation productivity under varied LMPs. As vegetation in IMAR has been reported to be degraded due to human activities, particularly overgrazing, many vegetation protection measures have been introduced[57]. For example, exclosure grazing excludes grazing from a protected area. Rotational grazing feeds animals in different fields in rotation depending on the forage condition. Both exclosure and rotational grazing are believed to be good strategies that have proved effective in protecting vegetation[58]. In addition, rest-grazing allows grazing fields to be rested and grazed on a rotational base. Reseeding is a measure to supplement grass seeds to improve vegetation density. These measures have also been proved to be OLMPs in the grassland. Those vegetation restoration measures have been implemented over the last two decades or so across the IMAR grasslands.

Grassland vegetation NPP can be quantified by the method using maximum peak live biomass[59]. A set of sites under the above-mentioned OLMPs, including exclosure grazing, rotational grazing, rest-grazing, and reseeding, have been selected across the pastoral counties in IMAR characterized by livestock grazing (Supplementary Fig. 10). Those sites under OLMPs are small fenced or protected areal patches. Vegetation productivities within and outside each site are compared to estimate the effectiveness of vegetation protection from the OLMPs. Within and outside each site stand for with and without implementation of the OLMPs, respectively. Aboveground biomass was collected in pairs, namely in and outside each protected area, at the time of peak vegetation growth in late August each year during 2009–2015, led by the Inner Mongolia Grassland Survey Institute. Estimating NPP from the maximum peak live biomass requires total biomass (the sum of aboveground and belowground).

Unfortunately, the belowground biomass is not included in the historical dataset. Previous studies conclude that the below-aboveground biomass ratio can

be used to estimate the belowground biomass. However, this biomass ratio in the grassland varies among different vegetation types. The below-aboveground biomass ratio (b_a_ratio) of meadow steppe, typical steppe, and desert steppe in IMAR was found to be 7.04, 5.16, and 5.32, respectively[60]. These ratio metrics are used to estimate belowground biomass for different grassland biomes types in this study. In addition, grazing animals consumed considerable biomass for sites outside the protected area, which must be considered. There is no detailed multi-temporal data about locations with varied grazing intensity. The biomass consumed by grazing animals is estimated using the livestock statistics data from the yearly statistical yearbook of IMAR for the pastoral counties. The livestock statistical data is spatially re-allocated based on the area of the counties. The numbers of different types of livestock are converted uniformly to the standard sheep units based on the consumption of forage. Each sheep unit averagely consumes 1.8 kg dry forage per day according to the national standard of calculation of rangeland carrying capacity (NY/T 635-2015, Agriculture Ministry of China 2015). The total biomass (T_BIO) gap between with and without OLMPs can be written as,

$$\mathrm{T\_BIO\_gap} = \max(0, \mathrm{T\_BIO_{in}} - \mathrm{T\_BIO_{out}}) \quad (5)$$

where $\mathrm{T\_BIO_{in}} = (1 + \mathrm{b\_a\_ratio}) \times \mathrm{A\_BIO_{in}}$ is the biomass density with OLMPs, and $\mathrm{A\_BIO_{in}}$ is the aboveground biomass. Similarly, $\mathrm{T\_BIO_{out}} = (1 + \mathrm{b\_a\_ratio}) \times \mathrm{A\_BIO_{out}} + 1.8 \times days \times sheep\_unit$, where $\mathrm{T\_BIO_{out}}$ and $\mathrm{A\_BIO_{out}}$ are the biomass density and the aboveground biomass density outside the OLMPs implemented area, respectively, *days* is the accumulated grazing days starting from the date of vegetation green-up, which was set from May 1, to the date of the field data collection, August 31, and *sheep_unit* is the grazing intensity in the sheep unit outside the site.

The relative increase in vegetation productivity attributed to the implementation of OLMPs, is the ratio of the biomass gap (T_BIO_map) to the total biomass outside each site ($\mathrm{T\_BIO_{out}}$, $\mathrm{T\_BIO_{out}} \neq 0$), which is formulated as,

$$\mathrm{Relative\_BIO\_gap} = \mathrm{T\_BIO\_map}/\mathrm{T\_BIO_{out}} \times 100\% \quad (6)$$

where the computed Relative_BIO_gap indicates the possible increase of biomass when OLMPs get implemented. Similarly, the ratio of the carbon gap to NPP reflects the relative increase in NPP if the identified OLMPs are implemented at a location, which takes the form as,

$$\mathrm{Relative\_Carbon\_gap} = \mathrm{Carbongap}/\mathrm{NPP} \times 100\% \quad (7)$$

A linear relationship between Relative_Carbon_gap and Relative_BIO_gap is computed to reflect their consistency. A moderate correlation between the estimated carbon gap and field observations was achieved, with $R^2$ 0.40 and a linear regression coefficient (β) 0.94 (Supplementary Fig. 11), which suggested good consistency between the estimated carbon gap and observed the increased potential of the grassland biomass.

## Data availability

The modeling results, in the form of the global carbon gap density and other report sheets, are available at https://doi.org/10.1594/PANGAEA.926334. The datasets used to compute the carbon gap for this study are publicly available, which has been described in "Methods".

## Code availability

The Python code for processing the carbon gap, code_wld_nature.py, is available for download from Pangea at https://doi.org/10.1594/PANGAEA.926334. This code works on Google Earth Engine.

Received: 9 April 2021; Accepted: 16 December 2021;
Published online: 18 January 2022

## References

1. Figueres, C. et al. Three years to safeguard our climate. *Nature* **546**, 593–595 (2017).
2. Adam, E. & Mutanga, O. Spectral discrimination of papyrus vegetation (Cyperus papyrus L.) in swamp wetlands using field spectrometry. *ISPRS J. Photogramm. Remote Sens.* **64**, 612–620 (2009).
3. Holden, P. B. et al. Climate-carbon cycle uncertainties and the Paris Agreement. *Nat. Clim. Chang.* **8**, 609–613 (2018).
4. Jackson, R. B. et al. Persistent fossil fuel growth threatens the Paris Agreement and planetary health. *Environ. Res. Lett.* **14**, (2019).
5. Peters, G. P. et al. Carbon dioxide emissions continue to grow amidst slowly emerging climate policies. *Nat. Clim. Change* **10**, 3–6 (2020).
6. Figueres, C. et al. Emissions are still rising: ramp up the cuts. *Nature* **564**, 27–30 (2018).
7. Aaron-Morrison, A. P. et al. State of the climate in 2014. *Bull. Am. Meteorol. Soc.* **96**, S1–S267 (2015).
8. Baldocchi, D., Ryu, Y. & Keenan, T. Terrestrial carbon cycle variability. *F1000Research* **5**, 2371 (2016).
9. Lal, R. et al. The carbon sequestration potential of terrestrial ecosystems. *J. Soil Water Conserv.* **73**, 145A–152A (2018).
10. Del Grosso, S. et al. Global potential net primary production predicted from vegetation class, precipitation, and temperature. *Ecology* **89**, 2117–2126 (2008).
11. Pan, S. et al. Modeling and monitoring terrestrial primary production in a changing global environment: toward a multiscale synthesis of observation and simulation. *Adv. Meteorol.* **2014**, 965936 (2014).
12. DeLucia, E. H. et al. Net primary production of a forest ecosystem with experimental $CO_2$ enrichment. *Science* **284**, 1177–1179 (1999).
13. Bond-lamberty, B. et al. Estimating heterotrophic respiration at large scales: challenges, approaches, and next steps. *Ecosphere* **7**, 1–13 (2016).
14. Wolf, S. et al. Warm spring reduced carbon cycle impact of the 2012 US summer drought. *Proc. Natl. Acad. Sci. USA* **113**, 5880–5885 (2016).
15. Baartman, J. E. M., Temme, A. J. A. M. & Saco, P. M. The effect of landform variation on vegetation patterning and related sediment dynamics. *Earth Surf. Process. Landforms* **43**, 2121–2135 (2018).
16. Sha, Z., Li, R., Li, J. & Xie, Y. Estimating carbon sequestration potential in vegetation by distance-constrained zonal analysis. *IEEE Geosci. Remote Sens. Lett.* 1–5. https://doi.org/10.1109/lgrs.2020.3003448 (2020).
17. Scurlock, J. M. O. & Olson, R. J. Terrestrial net primary productivity—a brief history and a new worldwide database. *Environ. Rev.* **10**, 91–109 (2002).
18. Erb, K. H. et al. Biomass turnover time in terrestrial ecosystems halved by land use. *Nat. Geosci.* **9**, 674–678 (2016).
19. Zhang, Y., Huang, K., Zhang, T., Zhu, J. & Di, Y. Soil nutrient availability regulated global carbon use efficiency. *Glob. Planet. Change* **173**, 47–52 (2019).
20. Erb, K. H. et al. Unexpectedly large impact of forest management and grazing on global vegetation biomass. *Nature* **553**, 73–76 (2018).
21. Arneth, A. et al. Historical carbon dioxide emissions caused by land-use changes are possibly larger than assumed. *Nat. Geosci.* **10**, 79–84 (2017).
22. Knoke, T. et al. Afforestation or intense pasturing improve the ecological and economic value of abandoned tropical farmlands. *Nat. Commun.* **5**, 1–12 (2014).
23. Tong, X. et al. Increased vegetation growth and carbon stock in China karst via ecological engineering. *Nat. Sustain.* **1**, 44–50 (2018).
24. Gonzalez-Roglich, M. et al. Synergizing global tools to monitor progress towards land degradation neutrality: trends.Earth and the World Overview of Conservation Approaches and Technologies sustainable land management database. *Environ. Sci. Policy* **93**, 34–42 (2019).
25. Hu, X., Zhang, L., Ye, L., Lin, Y. & Qiu, R. Locating spatial variation in the association between road network and forest biomass carbon accumulation. *Ecol. Indic.* **73**, 214–223 (2017).
26. UN-Habitat & International City Leaders. *2015 Global City Report*. https://smartnet.niua.org/content/ba3a1dcb-3012-44d6-87b5-fbaa28318de7 (2016).
27. Song, J. et al. The carbon sequestration potential of China's grasslands. *Ecosphere* **9**, e02452 (2018).
28. Alemseged, Y., Hacker, R. B., Smith, W. J. & Melville, G. J. Temporary cropping in semi-arid shrublands increases native perennial grasses. *Rangel. J.* **33**, 67–78 (2011).
29. Ramankutty, N. & Foley, J. A. Characterizing patterns of global land use: an analysis of global croplands data. *Global Biogeochem. Cycles* **12**, 667–685 (1998).
30. Liao, C., Luo, Y., Tang, X., Ma, Z. & Li, B. Effects of human population density on the pattern of terrestrial nature reserves in China. *Glob. Ecol. Conserv.* **20**, e00762 (2019).
31. Griscom, B. W. et al. Natural climate solutions. *Proc. Natl. Acad. Sci. USA* **114**, 11645–11650 (2017).
32. Tokarska, K. B. & Gillett, N. P. Cumulative carbon emissions budgets consistent with 1.5 °C global warming. *Nat. Clim. Chang.* **8**, 296–299 (2018).
33. Forsell, N. et al. Assessing the INDCs' land use, land use change, and forest emission projections. *Carbon Balanc. Manag.* **11**, 1–17 (2016). *2016 111.*
34. Gallagher, K. S., Zhang, F., Orvis, R., Rissman, J. & Liu, Q. Assessing the Policy gaps for achieving China's climate targets in the Paris Agreement. *Nat. Commun.* **10**, 1–10 (2019). *2019 101.*
35. Kulovesi, K. & Oberthür, S. Assessing the EU's 2030 Climate and Energy Policy Framework: incremental change toward radical transformation? *Rev. Eur. Comp. Int. Environ. Law* **29**, 151–166 (2020).
36. Dubash, N. K., Khosla, R., Rao, N. D. & Bhardwaj, A. India's energy and emissions future: an interpretive analysis of model scenarios. *Environ. Res. Lett.* **13**, 074018 (2018).
37. Chen, C. et al. China and India lead in greening of the world through land-use management. *Nat. Sustain.* **2**, 122–129 (2019).
38. Runck, B. C., Khoury, C. K., Ewing, P. M. & Kantar, M. The hidden land use cost of upscaling cover crops. *Commun. Biol.* **3**, 1–4 (2020). *2020 31.*

39. Yang, X. M., Drury, C. F., Reynolds, W. D. & Reeb, M. D. Legume cover crops provide nitrogen to corn during a three-year transition to organic cropping. *Agron. J.* **111**, 3253–3264 (2019).
40. Kemppinen, K. M. S. et al. Global reforestation and biodiversity conservation. *Conserv. Biol.* **34**, 1221–1228 (2020).
41. Change, G. & Sciences, B. Global mapping of terrestrial primary productivity and light-use efficiency with a process-based model. In *Global Environmental Change*. 343–358 (Terrapub, 2004).
42. Mitsch, W. J. et al. Tropical wetlands: seasonal hydrologic pulsing, carbon sequestration, and methane emissions. *Wetl. Ecol. Manag.* **18**, 573–586 (2009).
43. Gu, F. et al. Modeling the effects of nitrogen deposition on carbon budget in two temperate forests. *Ecol. Complex.* **7**, 139–148 (2010).
44. Serrano, O., Lavery, P. S., Rozaimi, M. & Mateo, M. Á. Influence of water depth on the carbon sequestration capacity of seagrasses. *Global Biogeochem. Cycles* **28**, 950–961 (2014).
45. Stumpner, E. B. et al. Sediment accretion and carbon storage in constructed wetlands receiving water treated with metal-based coagulants. *Ecol. Eng.* **111**, 176–185 (2018).
46. Díaz, F. J., Ogeen, A. T. & Dahlgren, R. A. Agricultural pollutant removal by constructed wetlands: implications for water management and design. *Agric. Water Manag.* **104**, 171–183 (2012).
47. Moore, I. D., Grayson, R. B. & Ladson, A. R. Digital terrain modelling: a review of hydrological, geomorphological, and biological applications. *Hydrol. Process.* **5**, 3–30 (1991).
48. Iwahashi, J. & Pike, R. J. Automated classifications of topography from DEMs by an unsupervised nested-means algorithm and a three-part geometric signature. *Geomorphology* **86**, 409–440 (2007).
49. Cao, M., Marshall, S. & Gregson, K. Global carbon exchange and methane emissions from natural wetlands: application of a process-based model. *J. Geophys. Res. Atmos.* **101**, 14399–14414 (1996).
50. Jones, P. G. & Thornton, P. K. Representative soil profiles for the Harmonized World Soil Database at different spatial resolutions for agricultural modelling applications. *Agric. Syst.* **139**, 93–99 (2015).
51. Gang, C. et al. Quantitative assessment of the contributions of climate change and human activities on global grassland degradation. *Environ. Earth Sci.* **72**, 4273–4282 (2014).
52. Adams, B., White, A. & Lenton, T. M. An analysis of some diverse approaches to modelling terrestrial net primary productivity. *Ecol. Modell.* **177**, 353–391 (2004).
53. Abatzoglou, J. T., Dobrowski, S. Z., Parks, S. A. & Hegewisch, K. C. TerraClimate, a high-resolution global dataset of monthly climate and climatic water balance from 1958-2015. *Sci. Data* **5**, 1–12 (2018).
54. Xu, S., Liu, Y., Wang, X. & Zhang, G. Scale effect on spatial patterns of ecosystem services and associations among them in semi-arid area: a case study in Ningxia Hui Autonomous Region, China. *Sci. Total Environ.* **598**, 297–306 (2017).
55. Tang, X. et al. Global patterns of soil heterotrophic respiration—a meta-analysis of available dataset. *CATENA* **191**, 104574 (2020).
56. Center for International Earth Science Information Network—CIESIN—Columbia University. 2018. Gridded Population of the World, Version 4 (GPWv4): Population Count Adjusted to Match 2015 Revision of UN WPP Country Totals, Revision 11. Palisades, NY: NASA Socioeconomic Data and Applications Center (SEDAC). https://doi.org/10.7927/H4PN93PB. Accessed 17 July 2020.
57. Mu, S. J. et al. Grassland dynamics in response to climate change and human activities in inner Mongolia, China between 1985 and 2009. *Rangel. J.* **35**, 315–329 (2013).
58. Dong, L. et al. Effect of grazing exclusion and rotational grazing on labile soil organic carbon in north China. *Eur. J. Soil Sci.* https://doi.org/10.1111/ejss.12952 (2020).
59. Ni, J. Estimating net primary productivity of grasslands from field biomass measurements in temperate northern China. *Plant Ecol.* **174**, 217–234 (2004).
60. Ma, W. H., Yang, Y. H., He, J. S., Zeng, H. & Fang, J. Y. Above- and belowground biomass in relation to environmental factors in temperate grasslands, inner Mongolia. *Sci. China, Ser. C Life Sci.* **51**, 263–270 (2008).


## Acknowledgements

This work was supported in part by the National Natural Science Foundation of China (Nos. 41871296 and 42171447). We acknowledge that the world population data comes from the Gridded Population of World (Ver. 4, from NASA Socioeconomic Data and Applications Center), and the MODIS data (NPP products and land-cover data) from NASA's Land Processes Distributed Active Archive Center (LP DAAC).

## Author contributions

Z.S., Y.X., Y.B., and R.L. conceived the modeling framework to estimating the carbon gap. Z.S. and H.L. realized (coded) the carbon gap modeling on Google Earth Engine and conducted the data analyses. Z.S. wrote the manuscript. Y.X., Z.S., and Y.B. revised the manuscript. X.Z., J.L., and X.L. participated in the modeling and computation. S.C. participated in the validation experiment. J.L. reviewed the data and results. All authors provided feedback on the manuscript.

## Competing interests

The authors declare no competing interests.

## Additional information

**Supplementary information** The online version contains supplementary material available at https://doi.org/10.1038/s43247-021-00333-1.

**Correspondence** and requests for materials should be addressed to Yichun Xie.

**Peer review information** *Communications Earth & Environment* thanks Maíra Padgurschi and the other, anonymous, reviewers for their contribution to the peer review of this work. Primary Handling Editors: Alessandro Rubino and Clare Davis. Peer reviewer reports are available.

**Reprints and permission information** is available at http://www.nature.com/reprints

**Publisher's note** Springer Nature remains neutral with regard to jurisdictional claims in published maps and institutional affiliations.